The PHEMU21 catalogue and astrometric results of the observations of the mutual occultations and eclipses of the Galilean satellites of Jupiter made in 2021

N. Emelyanov, J. -E. Arlot, P. Anbazhagan, P. André, J. Bardecker, G. Canaud, J. F. Coliac, J. de Elias Cantalapiedra, C. K. Ellington, J. M. Fernandez, et al.

Monthly Notices of the ROYAL ASTRONOMICAL SOCIETY

MNRAS **516,** 3685–3691 (2022)
Advance Access publication 2022 September 8

https://doi.org/10.1093/mnras/stac2538

The PHEMU21 catalogue and astrometric results of the observations of the mutual occultations and eclipses of the Galilean satellites of Jupiter made in 2021

N. Emelyanov,[1,2★] J.-E. Arlot,[2] P. Anbazhagan,[3] P. André,[4] J. Bardecker,[5] G. Canaud,[6] J. F. Coliac,[7] J. De Elias Cantalapiedra,[8] C. K. Ellington,[9] J. M. Fernandez,[10] M. Forbes,[11] K. Gazeas,[12] D. Gault,[13] T. George,[14] F. Gourdon,[15] D. Herald,[16] D. Huber,[17] R. Iglesias-Marzoa,[18] J. Izquierdo,[8] R. Jorba Lloveras,[8] S. Kerr,[16] A. Lasala,[19] P. Le Guen,[20] A. Leroy,[6] M. Lutz,[21] P. Maley,[22] T. Mannchen,[21] J. M. Mari,[17] A. Maury,[17,18] J. Newman,[16] S. Palafouta,[12] J. Prieto Gallego,[8] P. Roger,[15] D. Röschli,[23] G. Selvakumar,[3] V. Serra,[21] P. Stuart,[24] M. Turchenko,[1,25] R. Vasundhara[26] and E. Velasco[8,27]

Affiliations are listed at the end of the paper

Accepted 2022 September 2. Received 2022 September 2; in original form 2022 June 24

ABSTRACT

2021 was the year of Jupiter's equinox, that is the Sun and the Earth passed through the equatorial plane of the planet and therefore the orbital planes of its main satellites. This occurrence made it possible to observe mutual occultations and eclipses between the satellites. Our former experience shows that observations of such events provide accurate astrometric data that can be used to obtain new information on the dynamics of the Galilean satellites. The observations are a series of photometric measurements of a satellite which are carried out through the organization of a world wide campaign of observations thus maximizing the number and the quality of the data obtained. This work focuses on processing the photometric observations of the mutual occultations and eclipses of the Galilean satellites of Jupiter made during the international campaign in 2021. The final goal is to derive new accurate astrometric data. We used an accurate photometric model of mutual events in conjunction with the accuracy of observation. We obtained and processed the 84 light curves obtained during the campaign. As compared with the current best ephemerides, the rms of 'O–C' residuals are equal to 49 and 48 mas in right ascension and declination, respectively.

Key words: ephemerides – planets and satellites: general.

1 INTRODUCTION

Photometric observations of mutual occultations and eclipses of natural satellites of planets offer an efficient source of new astrometric data. Adding this new data makes it possible to significantly refine the model of the motion of Jupiter's satellites. It is from observations of mutual phenomena in the system of Galilean satellites that the secular acceleration of the moon Io was derived by Aksnes & Franklin (2001). It was concluded for the first time by the authors of this work that Io is losing more orbital energy from internal dissipation than it gains from Jupiter's tidal torque.

Refinement of the model of motion of the Galilean satellites based on observations was continued in (Lainey et al. 2009). Observations of the mutual occultations and eclipses of the Galilean moons occurring every six years from 1973 to 2003 were used. The observations of mutual events, known to be among the most accurate observations, have high accuracy and provide the best constraint of the satellite orbits for the past decades. Lainey et al. (2009) reported a new determination of the tidal dissipation in Io and Jupiter through its effect on the orbital motions of the Galilean moons. With these data the transport of the internally generated energy was analysed.

Likewise, strong tidal dissipation within Saturn and constraints on Enceladus thermal state were revealed by Lainey et al. (2012) from astrometry including the data obtained from photometric observations of Saturn's major moons during their mutual occultations and eclipses.

Related to this point, there have now been several missions to investigate Jupiter and its satellites (Pioneer, Voyager, Galileo, Juno) in addition to the flybys of Cassini and New Horizons, spanning a period of four decades. PHEMU campaigns make a significant addition to observational data through simple ground-based observations.

We have taken the opportunity to organize a worldwide observational campaign in 2021 to gather very accurate astrometric observations to support this study. We report these results here.

2 THE MUTUAL EVENTS

The Earth and the Sun cross the equatorial plane of Jupiter every six years, i.e. at the time of the Jovian equinox. The Jovian declinations of the Earth and the Sun then become zero and, since the orbital plane of the Galilean satellites is close to the equatorial plane of Jupiter, the satellites occult and eclipse each other.

The 2021 period was not favourable because the equatorial plane crossing occurred far from the opposition of Jupiter so that the Sun made the observations difficult; mostly they were made in twilight.

★ E-mail: 4emelia6@gmail.com

Table 1. Results of the past campaigns of observations.

Number of	1985	1991	1997	2003	2009	2015	2021
sites	28	56	42	42	74	75	29
light curves	166	374	292	377	457	609	84
observable events	248	221	390	360	237	442	192
observed events	64	111	148	118	172	236	40

In order to predict the dates of the observable events we used the L1 ephemerides from Lainey, Duriez & Vienne (2004), Lainey, Arlot & Vienne (2004) for the motion of the Galilean satellites.

Before 2021, several observational campaigns were completed during previous occurrences (Arlot et al. 1992, 1997, 2006, 2009, 2014; Saquet 2018). Table 1 presents the results derived for each campaign until the present one.

Since no thick atmosphere surrounds any of the Galilean satellites, the photometric observations of these phenomena are extremely accurate for astrometric purposes. The results previously obtained after similar observations of the Galilean satellites demonstrated that high-astrometric accuracy could be achieved, sometimes higher than 50 mas (Lainey et al. 2004).

This fact allowed us to provide data necessary to improve the theoretical models of the orbital motions and determine the tidal effects in the dynamics of the Galilean satellites through the measurement of a shift in longitude of the satellites; this demonstrates the signature of an acceleration in their motions.

3 THE PHEMU21 CAMPAIGN

We coordinated an international campaign of the photometric observations of the mutual occultations and eclipses of the Galilean satellites of Jupiter made in 2021 (PHEMU21, the acronym PHEMU derived from 'phénomènes mutuels') to acquire a significant amount of events. These events occurred in a short period of time, so a large number of observers located at a number of geographically separated sites were required in order not to miss events due to meteorological conditions and to get observations of different events at different longitudes.

For this campaign, 192 observable mutual events were computed. Unfortunately, the conjunction between Jupiter and the Sun occurred close to the Jovian equinox which provided the best opportunities for the occurrence of the events. Only 40 events were observed and a total of 84 light curves obtained. The declination of Jupiter was negative, so that the planet was low above the horizon for the observers of the northern hemisphere making their observations more difficult. Meteorological conditions were not favourable everywhere during this campaign.

3.1 Detectors

When observing mutual events, only relative photometry can generally be completed. Since the elevation of Jupiter above the horizon may be small, the airmass is often too high and absolute photometry is then impossible. Telescopes were equipped with 2D-detectors. Two kinds of detectors were used, the video cameras providing movies and the two-dimensional CCD or CMos detectors providing series of images. Visual observations and observations using a single channel photoelectric photometers were not conducted. Due to bad meteorological conditions and to the low elevation of Jupiter above the horizon in the Northern hemisphere, the photometric calibration was poor most of time, which resulted in the necessity to add some unknowns in the reduction equations.

3.2 Sites of observation

Coordinated by the SAI (Sternberg Astronomical Institute) and IMCCE (Institut de mécanique céleste et de calculs des éphémérides), this campaign included 29 sites of observations. The sites are given in Table 2 which lists the locations, codes, longitudes, latitudes, altitudes, the type of telescopes used (T means reflector, L refractor) followed by the aperture and focal distance in cm. The type of the detector (CCD or Video) is given in the last column.

To identify sites of observation with telescopes used, a special code is given for each of them. This code we name as the observatory code. It is to identify the sites and telescope given in the tables of photometric and astrometric results. These codes are the same in all tables.

So, we have 37 different systems of observation (telescope and detector) located at 29 sites in 11 countries.

4 LIGHTCURVES REDUCTION PROCEDURE

From each observation, which is a series of successive images coming from a video movie or from CCD or CMOS recordings, we deduced a light curve of the mutual occultation or eclipse of the satellites.

In all cases, each image must be dated in Universal Time or in a time-scale linked to Universal Time with an accuracy better than 0.1 s.

The photometry of each image had to be made with care even if we were doing relative photometry, not absolute. In order to perform relative photometry, each recording of an event must have either two objects on each image (usually, the occulted or eclipsed satellite with another reference satellite) or a reference object taken before and after the event if only the satellites involved in the event were present in the field. It is necessary that the reference object's flux should be constant during the event. If not, we conclude such appearance is due to the passage of light clouds. Then, the reference object was used to rebuild the fluxes by dividing event flux by the reference flux. For each moment, this ratio does not depend on any variation of the global received light flux. Also, the background light had to be removed especially for observations made during twilight when it varied rapidly.

Then, the light reflected by the satellites was measured on each image. For each observation, the following data were saved in a separate file: the dates in UTC and the light fluxes of the satellites involved in the event followed eventually by the light from a reference object and the light from the background. These files were provided by observers. However, in our data base, we provide reduced data, i.e. the flux of the occulted or eclipsed satellites corrected for absorption and sky background (see http://www.imcce.fr/fr/ephemerides/donnees/nsdc/nsdf/fjuphemu.html).

Figs 1 to 5 show examples of light curves. The points are the measured light flux and the line is the modelled flux of the predicted event fitted to the observations. Note that for each image, the determination of the light flux can be made either through a Gaussian fit of the object or an aperture photometry integrating all the light in a specific area with careful elimination of the sky background.

An example of the photometric data is given in the Table 3.

5 EXTRACTION OF ASTROMETRIC DATA FROM PHOTOMETRY OF MUTUAL OCCULTATIONS AND ECLIPSES OF SATELLITES

Let us consider now the method for inferring positional and astrometric data from the measurements of satellite fluxes during their mutual

Table 2. Sites of observation for the PHEMU21 campaign. The column 'altitude' gives the value of the altitude if the observatory is not included in the IAU list of observatories. Otherwise, the code of the observatory (in brackets) is given according to the IAU list, where the altitude is not given. If the IAU code is given then geocentric latitude is meant else this is astronomical latitude given by observers.

Location of observatory	codes	East longitude, (°)	latitude, (°)	Altitude, m	Tel.	D, cm	f, cm	Detector
Sainte Foy d'Aigrefeuille, Fr	SFA	1.610278	43.544167	163	T	20	100	CCD
Aurin, Fr	AUR	1.690555	43.540833	241	T	20	100	CCD
Gretz-Armainvilliers, Fr	URA	2.744400	48.551901	(A07)	T	25	250	CCD
Ygrande, Fr	YGR	2.944444	46.552778	330	T	11	100	CCD
Toulon, Fr	OAG	5.340278	43.150555	200	T	20	80	Video
La Seyne sur Mer, Fr	SEY	5.861111	43.058889	132	T	20	80	Video
Toulon, Fr	BAF	5.896111	43.155555	200	L	10	53	CCD
Toulon, Fr	BAO	5.896111	43.155555	200	L	10	164	CCD
Toulon, Fr	BAU	5.896111	43.155555	200	L	20	200	CCD
Le Mont Caume, Fr	CAU	5.899811	43.182869	706	T	20	80	Video
Selfkant, Germany	MEA	5.933889	51.039694	52	T	25	254	Video
Antibes, Fr	TLV	7.005200	43.417246	(G14)	T	35	391	CCD
Cademario, Switzerland	CAD	8.899811	46.019964	755.3	T	18	150	CCD
KGO SAI, Russia	KGO	42.672203	43.738130	2073	T	35	160	CCD
Murrumbateman, Australia	E07	148.998890	− 34.778198	(E07)	T	40	400	Video
Flynn, Australia	FLY	149.049313	− 35.198705	657	T	35	224	Video
Glenlee, Australia	GLE	150.500444	− 23.130109	(Q70)	T	30	300	CCD
Kuriwa, Australia	KUR	150.641110	− 33.664579	(E28)	T	30	150	CCD
New Zealand	MRR	174.974310	− 41.160555	26	T	20	780	Video
Gardnerville Nevada USA	GAR	240.327694	38.889861	1524	T	30	305	Video
Gardnerville Nevada USA	GA2	240.327694	38.889861	1524	T	30	305	CCD
Carefree, Arizona USA	PAU	248.047780	33.811944	0	T	20	200	Video
Granite Peak Trail, Scottsdale, Arizona US,	GRA	248.131306	33.816694	830	T	30	99	Video
Stuart dome, Texas USA	PSD	264.964839	29.548753	16	T	20	92	Video
San Pedro de Atacama, Chile	SPA	291.82019	− 22.815249	(W94)	L	25	200	CCD
Sevilla, Spain	SEV	354.019097	37.393261	63	T	5	200	CCD
AAM, Madrid, Spain	L46	356.11939	40.270973	(L46)	L	20	200	CCD
Miraflores, Spain	MRF	356.243069	40.811955	1137	T	20	102	CCD
Madrid, Spain	CRQ	356.508556	40.794778	690	T	20	160	CCD
Madrid, Spain	SRD	356.327750	40.549305	787	T	20	160	CCD
Madrid, Spain	XXX	356.328333	40.549167	734	T	12	90	CCD
Madrid, Spain	MAD	356.338889	40.449167	720	T	13	100	CCD
Zaragoza, Spain	MRJ	358.517944	41.474194	410	T	28	280	CCD
Javalambre Observatory, Spain	OAJ	358.983508	40.042630	1957	T	40	360	CCD
University of Athens, Greece	UNV	23.783333	37.968555	250	T	40	320	CCD
Vainu Bappu Observatory, India	VBO	78.826300	12.494750	(220)	T	130	1040	CCD

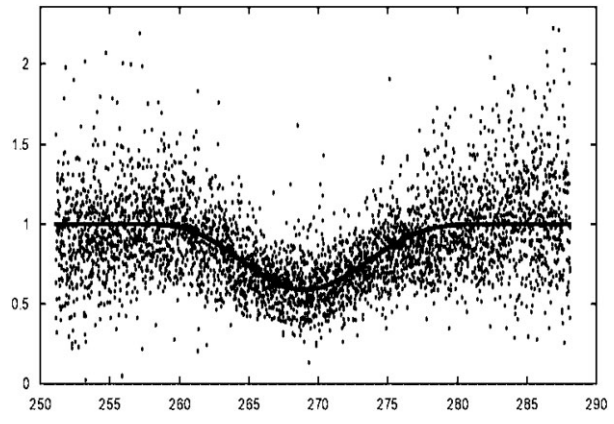

Figure 1. J1 eclipses J4 on 2021 April 12: this observation shows an event for which the predicted magnitude drop is close to the calculated one. The signal is noisy because of the large number of points and the small integrating time.

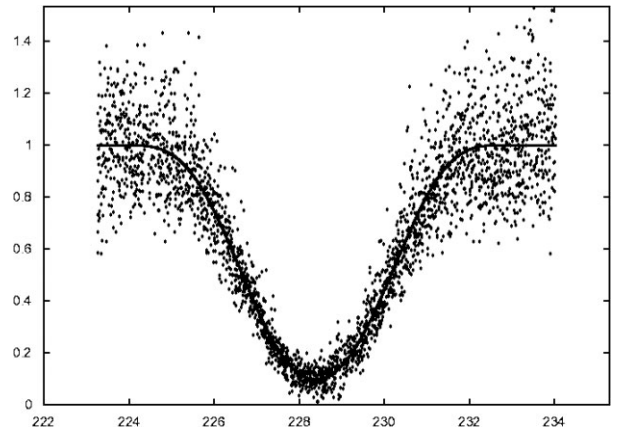

Figure 2. J3 eclipses J1 on 2021 May 14. The signal is noisy due to the bad seeing. Note that the magnitude drop may come close to 100 per cent only in case of an eclipse.

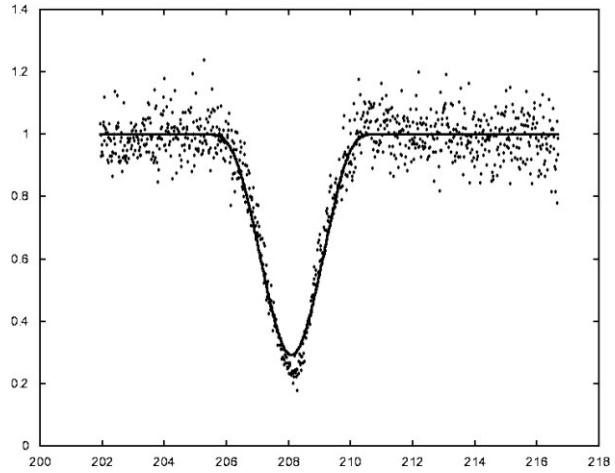

Figure 3. J1 eclipses J2 on 2021 May 6: the model did not fit the observation well. This is due to a defect in the calibration or a wrong value taken for the albedo of the eclipsed satellite.

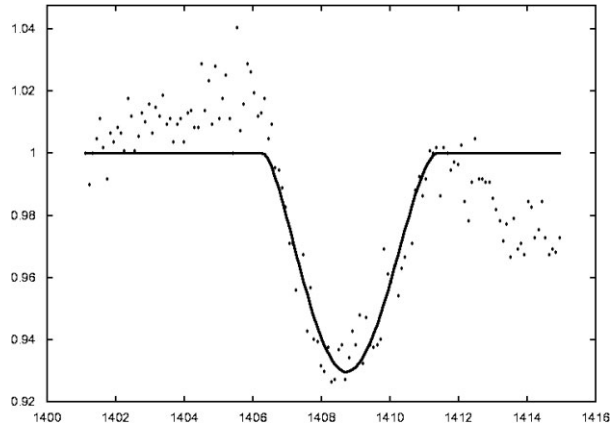

Figure 4. J2 occults J3 on 2021 April 12: we have here a small magnitude drop. Just after the end of the event, the absorption of the sky is too large and the signal decreases.

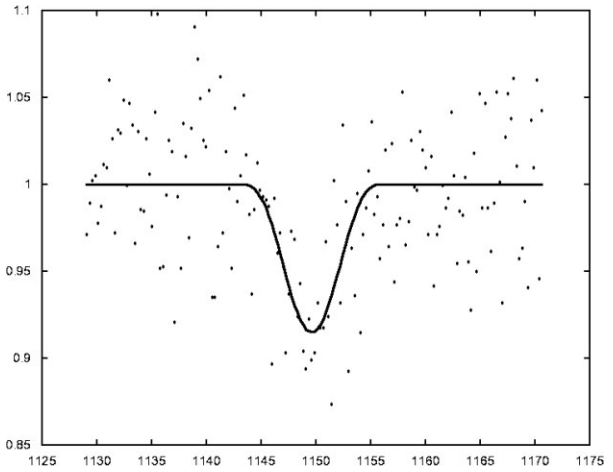

Figure 5. J3 eclipses J2 on 2021 August 30: a grazing event showing a very faint magnitude drop.

Table 3. Fragments of the photometric measurement file corresponding to the data in Fig. 1. J1 eclipses J4 on 2021 April 12. The moments are given in UTC scale counted from 0 h of the observation date.

Moment, min	Normalzed measured light flux	Model light flux
251.08260	1.561563	1.000000
251.09093	0.415533	1.000000
251.10760	0.636040	1.000000
–	–	–
268.41940	0.399085	0.592393
268.42774	0.455998	0.592289
268.44440	0.651969	0.592085
–	–	–
282.13881	1.185483	0.999999
282.14715	1.099906	0.999999
282.15549	1.000674	1.000000
...	–	–

occultations and eclipses. We followed the procedure described in (Emel'yanov 2003; Emelyanov & Gilbert 2006). According to this method, we used a value S presenting the normalized flux coming from the observed satellites during the event. Thus $S = 1$ for all time instants before and after the event and $S < 1$ due to the mutual occultation or eclipse.

Then we considered the projections $X_c(t)$ and$Y_c(t)$ of the differences of planetocentric Cartesian coordinates of the two satellites on to the plane of the event. In the case of mutual occultations, this plane coincides with the plane passing through the occulted satellite perpendicular to the line of sight of the observer. In the case of a mutual eclipse, the plane of the event passes through the eclipsed satellite perpendicular to the line connecting the satellite with the centre of the Sun. The coordinate origin is placed at the centre of the *passive* (occulted or eclipsed) satellite. The occulting or eclipsing satellite is referred to as the *active* satellite.

Given the topocentric distances of the active and passive satellites, one can compute the corresponding projections $X(t)$ and $Y(t)$ of the angular separation between the satellites on to the celestial parallel and meridian, respectively. It goes without saying that the topocentre is taken to coincide with the centre of the Sun in the case of a mutual eclipse. The time instants for which the positions of the satellites are determined do not coincide with the time of observation. The relations between these time instants can be found in Emelyanov (2020).

So the value S is to be written as a function $S(X(t), Y(t))$.

Let E_i be the photometric count made at the moment t_i. Here m is the number of photometric counts during a single event. With appropriate theories of motion of planets and satellites, one can compute for the moment t_i ($i = 1, 2, \ldots, m$) of each photometric measurement the theoretical values of functions $X(t)$, $Y(t)$, i.e. $X_{\rm th}(t_i)$, $Y_{\rm th}(t_i)$. The real values of $X(t), Y(t)$ differ from $X_{\rm th}(t_i), Y_{\rm th}(t_i)$ by corrections D_x, D_y, i.e.

$$X(t) = X_{\rm th}(t_i) + D_x, \quad Y(t) = Y_{\rm th}(t_i) + D_y.$$

The underlying assumption of the method is that corrections D_x, D_y remain constant during the observed event. According to our estimates, the error introduced by this assumption for Galilean satellites does not exceed 3.7 km in the satellite coordinates. To achieve better accuracy, corrections D_x, D_y should be fitted by linear functions of time. In this case, the error should not exceed 0.025 km. The results of the reduction of modern observations show that with the actual errors of the satellite coordinates, the corrections D_x, D_y can be considered as constant.

Hereafter, we refer to the part of the photometric count that is not due to the satellite flux as the 'background', and denote it as B.

Our proposed method consists in solving conditional equations

$$E_i = K\ S(X_{\rm th}(t_i) + D_x, Y_{\rm th}(t_i) + D_y) + B \qquad (i = 1, 2, \ldots, m)$$

for the constants D_x, D_y, K, and B.

We linearized conditional equations with respect to parameters D_x, D_y and then solved them using the least squares method. This process is hereafter referred to as 'fitting the lightcurve'.

The astrometric result of the reduction of photometric observations of a single event can be taken to consist of the following values:

$$X = X(t^*) = X_{\rm th}(t^*) + D_x, \quad Y = Y(t^*) = Y_{\rm th}(t^*) + D_y,$$

where t^* is an arbitrary time instant inside the event interval. For the sake of definitiveness, we assumed that it is the time instant when $\sqrt{X^2 + Y^2}$ takes its minimum value, i.e. t^* is the time of the closest apparent approach of the satellites.

If the same event was observed at two observatories, the time instants t^* may differ because of observational errors, and the differences between X and Y obtained at two observatories cannot be viewed as bias indicators. However, the corrections D_x and D_y remain constant during the event and characterize the discrepancy between the theory and observations. The values obtained from observations made at different observatories can be compared to each other. The resulting discrepancies are due to observational biases.

Hereafter, we call the constants D_x, D_y, K, and B as the event parameters. So the parameters D_x, D_y are the differences between the astrometric coordinates $X = X(t^*) = X_{\rm th}(t_i) + D_x$, $Y = Y(t^*) = Y_{\rm th}(t_i) + D_y$ of the satellite corresponding to the observed light curve and the ephemeris coordinates $X_{\rm th}(t_i)$, $Y_{\rm th}(t_i)$. They are designated below as $(O - C)_x$ and $(O - C)_y$, correspondingly.

The internal accuracy of photometry as estimated from the least squares method is characterized by the errors σ_X and σ_Y of the inferred parameters X arcsec and Y arcsec. The estimates σ_X and σ_X are due to the random errors of the photometry only. They are called below as the standard deviation after ftting the light curve. A light curve may contain also some systemtic errors entering the values of the derived parameters D_x, D_y, B.

Our analysis lead us to the following two important conclusions. First, joint least squares determination of four parameters D_x, D_y, K, and B may result in highly correlated parameter errors, and the differences between the inferred parameters and their real values may substantially exceed the random errors. That is why it is better not to treat parameter B (background) as an unknown, but eliminate the effect of the background on the result of measurement in advance setting $B = 0$. Second, if we set $B = 0$ but eliminate the background incorrectly so that this parameter actually differs from zero, an unaccounted systematic error appears in parameter D_y.

There are light curves with flat bottoms although predictions show a dip drop below the flat bottom. After fitting the parameters of the model of the phenomenon, agreement can be established. In some cases, however, the discrepancy remains. This may be due to the aforementioned systematic errors in the measurements. Such effects are discussed in (Emelianov 2017). See also in the book Emelyanov (2020) (Chapter 7).

It is worth paying attention to the phenomenon that took place on 2021 April 19. During the 4e3 eclipse from 18h 32m to 18h 46m, the satellite J3 Ganymede also fell into the shadow of the satellite J1 Io. In order to correctly use the measured phenomenon 4e3, we excluded from the measurements, the model flux drop due to the shadow from J1 Io. Around the same period, the satellite J1 Io fell into the shadow of Callisto. However, the satellite J1 Io was at an apparent distance from J3 Ganymede and this phenomenon was not measured.

6 THE CATALOGUE

6.1 The data

The catalogue of the data gathered after the campaign of observations of the mutual events of the Galilean satellites is provided in the form of 84 files (one for each observation) containing a series of photometric measurements: the light curve obtained from the photometry of the mutual event calibrated using the flux scale coefficient K obtained after the fit of the parameters to the observation, so that the measured flux must be equal to 1 when no event occurs and to 0 if no light is received from the observed objects (if the flux was measured only from the eclipsed satellite or if the satellite has disappeared). The calibrated value of the measured flux is supplied with the theoretical value of the flux obtained after the fit of the parameters to the observation. Each line of the file gives three numbers: time in minutes counted from 0 h (UTC) of the date of the event, the calibrated value of the observed measured flux (the value E_i/K, see equation 2) and the light flux modelled after the fit of the parameters to the observation as explained above [the value $S(X_{\rm th}(t_i) + D_x, Y_{\rm th}(t_i) + D_y)$ in equation 2].

A file containing the relative astrometric positions of the two satellites involved in each mutual event (one line per event) as described in section 6.2 and in Tables 4 and 5.

Figs 1 to 5 show examples of observed light curves: the dots are the observations and the line is the model as explained in Sections 4 and 5.

The light curves and the astrometric results are available for anyone interested from the electronic data base of the Natural Satellite Data Center (NSDC) server.[1]

6.2 Astrometric results

We subdivide our final astrometric results into two groups. The first group includes the results obtained from the observations where two coordinates $X(t^*)$, $Y(t^*)$ arcsec could be successfully determined. The second group contains the results obtained in the cases where only position angle could be determined.

In the first group, each final result of the observation of a single mutual phenomenon at a given observatory is presented by the following fields: the date, the type of the phenomenon (eclipse or occultation) including the satellite numbers, the observatory code, the time instant t^* in the UTC scale, $X(t^*)$ arcsec, $Y(t^*)$ arcsec, σ_x, σ_y, D_x, and D_y arcsec. The type of phenomenon is coded as $n_a o n_p$ or $n_a e n_p$ for a mutual occultation or eclipse, respectively. Here n_a is the number of the occulting or eclipsing satellite and n_p is the number of the occulted or eclipsed satellite. We give the results in the form of the angular separation s (in arcsec) and position angle A (in degrees) corresponding to $X(t^*)$, $Y(t^*)$ arcsec.

The angular separation s is determined by the equation

$$s = \sqrt{(X\ \text{arcsec})^2 + (Y\ \text{arcsec})^2}.$$

[1] at the web address http://nsdb.imcce.fr/obsphe/obsphe-en/fjuphemu.html or on the ftp server at ftp://ftp.imcce.fr/ pub/NSDC/ jupiter/raw_data/phenomena/mutual/2021/ and at http://www.sai.msu.ru/neb/nss/index.htm

Table 4. Fragment of the first group of astrometric results.

Date yr, m., d.	Ty-pe	Obs. code	UTC Time h, m, s,	$X(t^*)$ arcsec	$Y(t^*)$ arcsec	σ_x arcsec	σ_y arcsec	D_x arcsec	D_y arcsec	s arcsec	A (°)	Q	$S_{\min}$
2021 6 14	1e2	CRQ	3 56 15.33	0.2941	− 0.7640	0.0515	0.0228	− 0.0031	0.0048	0.8186	158.945	0	0.9408
2021 6 14	1e2	L46	3 56 13.28	0.2969	− 0.7713	0.0551	0.0249	− 0.0108	− 0.0065	0.8264	158.945	0	0.9454
2021 6 14	1e2	MAD	3 56 4.39	0.2853	− 0.7411	0.0994	0.0241	− 0.0682	0.0060	0.7941	158.946	0	0.9258
...													
2021 8 30	3e2	OAG	19 9 45.16	0.3939	− 0.9038	0.0317	0.0183	0.0472	0.0888	0.9859	156.452	0	0.8845
2021 8 30	3e2	KGO	19 8 34.02	0.4264	− 0.9783	0.0134	0.0069	− 0.0723	− 0.0520	1.0672	156.449	0	0.9427
2021 8 30	3e2	UNV	19 9 37.50	0.4094	− 0.9393	0.0514	0.0264	0.0463	0.0461	1.0247	156.452	0	0.9151

Table 5. Fragment of the second group of astrometric results.

Date yr, m., d.	Ty-pe	Obs. code	UTC Time h, m, s,	A deg	σ_{along} arcsec	$(O-C)_{\text{along}}$ arcsec	R
2021 4 12	1e4	AUR	4 27 49.03	160.272	0.0126	0.1964	0
2021 4 19	4e3	GLE	18 38 53.24	160.549	0.0109	0.0724	0
...							
2021 5 29	3e1	OAG	2 50 4.57	340.002	0.0020	0.0273	0
2021 5 29	3e1	MAD	6 51 6.02	338.821	0.0095	0.0764	0

We also give the minimum level $S_{\min}$ of normalized flux. We assign flag Q to each observation in order to indicate the quality and the reliability of the result. Flag Q may take one of the following four values: '0' for normally determined coordinates, '1' for the cases where either photometric data are doubtful, or the result was obtained from low-quality photometry, or it significantly differs from that obtained at another observatory. Right ascensions and declinations are measured in the International Celestial Reference Frame (ICRF). All angular quantities are in arcseconds. In the case of a mutual occultation, t^* is the time of topocentric observation of satellites. For mutual eclipses, t^* is the time of topocentric observation of the eclipsed satellite.

The σ_x and σ_y quantities can be interpreted as internal errors of $\Delta\alpha \cos\delta_p$ and $\Delta\delta$, respectively, and D_x, D_y arcsec are the residuals with respect to the theory of Lainey et al. (2009).

Table 4 gives a fragment of the first section of astrometric results.

The data in the second group are presented by the following fields: the date, the type of the phenomenon (eclipse or occultation) including the satellite numbers, the code of the observatory, the time instant t^* in the UTC scale, the position angle A, the precision σ_{along} of the apparent position along the apparent relative trajectory of the satellite as obtained with the least-square method.

Differences in the apparent relative position of the satellites along the apparent relative trajectory obtained from observation and determined from the theory of Lainey et al. (2009) are given in the column $(O-C)_{\text{along}}$.

In addition, a flag R is assigned showing the reason why only one coordinate was determined: '0' for a total mutual eclipse or occultation observed, '1' for the results arising from low-quality photometry. In these cases, the apparent relative position of the satellite measured across the apparent trajectory can not be determined accurately enough and therefore position angles can be determined only up to $\pm 180^\circ$ ($A \pm 180^\circ$).

Table 5 gives a fragment of the the second group of the astrometric results.

Tables 4 and 5 are available in electronic form from Natural Satellites Data Center service at http://nsdb.imcce.fr/obsphe/obsphe-en/fjuphemu.html and http://www.sai.msu.ru/neb/nss/index.htm.

Table 6. Estimates of the accuracy of the results of astrometric reduction performed to determine two relative coordinates of satellites $X(t^*)$, $Y(t^*)$ arcsec. Only the 66 best observations are taken into account.

Type of total error estimates	Errors of X arcsec (in RA) mas	Errors of Y arcsec (in DEC) mas
Total random errors	33	24
R.m.s. of O–C from Lainey et al. (2009)	49	48

7 ESTIMATION OF THE ACCURACY OF THE DERIVED ASTROMETRIC RESULTS

The following estimates of the accuracy of the derived astrometric results were made. The least-squares method yields standard errors σ_x, σ_y for the parameters D_x, D_y arcsec derived from the observed light curves. These errors are due to random errors of photometry and characterize the internal accuracy of astrometric results. We have calculated the r.m.s. values of these estimates for the 66 best astrometric results taken with $Q = 0$. These estimates are listed in the Table 6 as total random errors.

The values $D_x$and D_y arcsec show an agreement of the theory by Lainey et al. (2009) with the obtained astrometric results. The values D_x arcsec are residuals in right ascension (RA) and D_y arcsec in declination (DEC). Therefore we have also calculated the total r.m.s. of all D_x and D_y arcsec computed over the 66 best observations mentioned above. These estimates are given in Table 6 as r.m.s. of O–C.

8 CONCLUSIONS

We reduced the entire data base of photometric observations of the mutual occultations and eclipses of the Galilean satellites of Jupiter made during the international campaign in 2021 to determine the topocentric or heliocentric angular differences for satellites pairs at 76 time instants within the time interval from 2021 February 28 to 2021 August 30.

The standard errors of the relative satellite coordinates due to the random errors of the photometry are equal to 33 and 24 mas in right ascension and declination, respectively. For successful observations, the r.m.s. of 'O–C' residuals with respect to the theory by Lainey et al. (2009) are equal to 49 and 48 mas in right ascension and declination, respectively. For eight observations the position angle only was derived.

The next opportunity for an observational campaign will be in 2025 for the Saturnian satellites and in 2026–27 for the Jovian satellites. Ephemerides of these events with local observational conditions are available at the addresses: http://nsdb.imcce.fr/multisat/nsszph6he.htm and http://www.sai.msu.ru/neb/nss/html/multisat/nsszph6he.htm

ACKNOWLEDGEMENTS

This work was supported by The European contract ESPaCE (FP7-grant agreement 263466), the Scientific Council of Paris Observatory, and the Programme National de Planetologie (CNES and CNRS).

Partially based on observations made with the Tx40 telescope at the Observatorio Astrofísico de Javalambre in Teruel, a Spanish Infraestructura Cientifico-Técnica Singular (ICTS) owned, managed, and operated by the Centro de Estudios de Física del Cosmos de Aragón (CEFCA). Tx40 is funded with the Fondos de Inversiones de Teruel (FITE).

Photometric data on mutual occultation event which occurred on 2021 August 30, were collected with the robotic and remotely controlled observatory at the University of Athens Observatory – UOAO (Gazeas 2016).

DATA AVAILABILITY

The data reported in this paper are available at the MULTI-SAT service elaborated by SAI and IMCCE (See authors' affiliations) accessible online at http://www.imcce.fr/fr/ephemerides/donnees/nsdc/nsdf/fjuphemu.html and http://www.sai.msu.ru/neb/nss/index.htm request.to the service MULTISAT described in the corresponding papers by SAI and IMCCE

REFERENCES

Aksnes K., Franklin F. A., 2001, AJ, 122, 2734
Arlot J. E. et al., 1992, A&AS, 92, 151
Arlot J. E. et al., 1997, A&AS, 125, 399
Arlot J. E. et al., 2009, A&A, 493, 1171
Arlot J.-E. et al., 2006, A&A, 451, 733
Arlot J.-E. et al., 2014, A&A, 572, A120
Dias-Oliveira A. et al., 2013, MNRAS, 432, 225
Emel'yanov N. V., 2003, Solar System Research, 37, 314
Emelianov N., 2017, Proc. Workshop and colloquium, Astrometry/photometry of Solar System objects after Gaia. 25
Emelyanov N., 2020, The Dynamics of Natural Satellites of the Planets. Elsevier, Amsterdam
Emelyanov N. V., Gilbert R., 2006, A&A, 453, 1141
Emelyanov N. V. et al., 2011, Solar System Research, 45, 264
Gazeas K., 2016, Rev. Mex. Astron. Astrofís., 48, 22
Lainey V. et al., 2012, ApJ, 752, 14
Lainey V., Duriez J. E., Vienne A., 2004a, A&A, 420, 1171
Lainey V., Arlot J. E., Vienne A., 2004b, A&A, 427, 371
Lainey V., Arlot J. E., Karatekin O., van Hoolst T., 2009, Nature, 459, 957
Saquet E. et al., 2018, MNRAS, 474, 4730

[1]*Sternberg Astronomical Institute, Lomonosov Moscow State University, Russia*
[2]*Institut de mécanique céleste et de calcul des éphémérides-Observatoire de Paris, PSL, UMR 8028 CNRS, UPMC, USTL, 77 avenue Denfert-Rochereau, F-75014 Paris, France*
[3]*Vainu Bappu Observatory, Indian Institute of Astrophysics, 635701 Kavalur, Tamil Nadu, India*
[4]*IOTA-ES, Société Astronomique de France, Adagio Belesta Observatory, Club d'astronomie de Quint-Fonsegrives, F-31570 Sainte Foy d'Aigrefeuille, France*
[5]*IOTA, Gardnerville, Nevada, USA*
[6]*Uranoscope de l'Ile de France, F-77220 Gretz-Armainvilliers, France*
[7]*OABAC : Observatoire pour l'Astronomie des Binaires et l'Astronomie Collaborative, Marseille, France*
[8]*Agrupación Astronómica de Madrid, E-28029 Madrid, Spain*
[9]*Maastricht Science Programme, NL-6229 Maastricht, Netherlands*
[10]*Astronomía Sevilla, Seville, Spain*
[11]*Occultation section RASNZ, Manor Park Observatory,, Lower Hutt 5019, New Zealand*
[12]*Section of Astrophysics, Astronomy and Mechanics, Department of Physics, National and Kapodistrian University of Athens, GR-15784 Zografos, Athens, Greece*
[13]*22 Booker Road, Hawkesbury Heights, N.S.W. 2777, Australia*
[14]*IOTA, Scottsdale, AZ USA*
[15]*OAGC Observatoire Astronomique du Gros Cerveau, Rte du Gros Cerveau F-83190 Ollioules, France*
[16]*Trans-Tasman Occultation Alliance, Murrumbateman Observatory, Australia*
[17]*GAPRA, F-06160 Antibes-Juan-les-Pins, France*
[18]*Centro de Estudios de Física del Cosmos de Aragón, Javalambre Astrophysical Observatory, E-44001, Teruel, Spain*
[19]*AAHU, Astronomical group of Huesca, Zaragoza, Spain*
[20]*Observatoire du Pic des Fées, 26 bis All. des Pinsons, F-83400 Hyères, Toulon, France*
[21]*Baden-Wuerttemberg Cooperative State University (DHBW) Ravensburg Campus Friedrichshafen; Fallenbrunnen 2, D-88045 Friedrichshafen, Germany*
[22]*IOTA and NASA Johnson Space Center Astronomical Society, Carefree, AZ, USA*
[23]*Cademario Observatory, Switzerland*
[24]*International Occultation Timing Association (IOTA), Fountain Hills, AZ 85269, USA*
[25]*Caucasian Mountain Observatory of the SAI of Moscow State University, Karachay-Cherkess Republic, Kichi-Balyk village, 369388 Russia*
[26]*Indian Institute of Astrophysics, Bangalore 560034, Karnataka, India*
[27]*Department of Theoretical Condensed Matter Physics, Facultad de Ciencias, Universidad Autonoma de Madrid,, E-28049 Madrid, Spain*

This paper has been typeset from a TEX/LATEX file prepared by the author.